Inorganic Chemistry Article

Inorg. Chem. **2010**, *49*, 123–135 **123**
DOI: 10.1021/ic901510m

Cooperation between Cis and Trans Influences in *cis*-$Pt^{II}(PPh_3)_2$ Complexes: Structural, Spectroscopic, and Computational Studies

Luca Rigamonti,[†] Alessandra Forni,[*,‡] Mario Manassero,[*,§] Carlo Manassero,[§] and Alessandro Pasini[*,†]

[†]*Università degli Studi di Milano, Dipartimento di Chimica Inorganica, Metallorganica e Analitica "Lamberto Malatesta", via Venezian 21, 20133 Milano, Italy,* [‡]*ISTM-CNR, via Golgi 19, 20133 Milano, Italy, and* [§]*Università degli Studi di Milano, Dipartimento di Chimica Strutturale e Stereochimica Inorganica, via Venezian 21, 20133 Milano, Italy*

Received July 29, 2009

The relevance of cis and trans influences of some anionic ligands X and Y in *cis*-$[PtX_2(PPh_3)_2]$ and *cis*-$[PtXY(PPh_3)_2]$ complexes have been studied by the X-ray crystal structures of several derivatives (X_2 = $(AcO)_2$ (**3**), $(NO_3)_2$ (**5**), Br_2 (**7**), I_2 (**11**); and XY = Cl(AcO) (**2**), $Cl(NO_3)$ (**4**), and $Cl(NO_2)$ (**13**)), density functional theory (DFT) calculations, and one bond Pt−P coupling constants, $^1J_{PtP}$. The latter have allowed an evaluation of the relative magnitude of both influences. It is concluded that such influences act in a cooperative way and that the cis influence is not irrelevant when rationalizing the $^1J_{PtP}$ values, as well as the experimental Pt−P bond distances. On the contrary, in the optimized geometries, evaluated through B3LYP/def2-SVP calculations, the cis influence was not observed, except for compounds ClPh (**21**), Ph_2 (**22**), and, to a lesser extent, $Cl(NO_2)$ (**13**) and $(NO_2)_2$ (**14**). A natural bond order analysis on the optimized structures, however, has shown how the cis influence can be related to the s-character of the Pt hybrid orbital involved in the Pt−P bonds and the net atomic charge on Pt. We have also found that in the X-ray structures of *cis*-$[PtX_2(PPh_3)_2]$ complexes the two Pt−X and the two Pt−P bond lengths are different each other and are related to the conformation of the phosphine groups, rather than to the crystal packing, since this feature is observed also in the optimized geometries.

Introduction

A fundamental aspect of coordination chemistry is the understanding of the influence that a ligand L, in an MLL'_n complex, exerts on the properties of the M−L′ bonds, because a knowledge of these influences can give an insight into aspects like stability and reactivity of the complexes under study. In the case of square planar and octahedral complexes, such influences are termed cis and trans influences, depending on which bond is influenced by the "influencing" ligand L.[1] The comprehensive importance of these aspects is shown by the fact that, in addition to the multitude of studies performed on transition metal complexes, there are examples also in main group chemistry.[2]

According to an original definition,[1,3] the trans influence of a ligand is related to the extent to which such ligand weakens the bond trans to itself in the ground state of the complex. The cis influence can be defined, similarly, as the weakening of a metal−ligand bond induced by a cis ligand. Several techniques have been employed to investigate these influences,[4] the most popular being X-ray crystallography[2a,4,5] ("structural" trans or cis influence) and NMR spectroscopy. The latter has been used extensively[6] when both the metal and the donor atoms are NMR active (such as, in the present case, ^{195}Pt and ^{31}P) by examining the ^1J values,

*To whom correspondence should be addressed. E-mail: alessandro.pasini@unimi.it (A.P.), a.forni@istm.cnr.it (A.F.), mario.manassero@unimi.it (M.M.).

(1) Pidcock, A.; Richards, R. E.; Venanzi, L. M. *J. Chem. Soc.* (*A*) **1966**, 1707–1710.
(2) (a) Ochiai, M.; Sueda, T.; Miyamoto, K.; Kiprof, P.; Zhdankin, V. V. *Angew. Chem., Int. Ed.* **2006**, *45*, 8203–8206. (b) Shustorovich, E. M.; Buslaev, Yu. A. *Inorg. Chem.* **1976**, *15*, 1142–1147.
(3) Venanzi, L. M. *Chem. Brit.* **1968**, *4*, 162–167.
(4) Appleton, T. G.; Clark, H. C.; Manzer, L. E. *Coord. Chem. Rev.* **1973**, *10*, 335–422.
(5) (a) Kukushkin, V. Yu.; Belsky, V. K.; Konovalov, V. E.; Kirakosyan, G. A.; Konovalov, L. V.; Moiseev, A. I.; Tkachuk, V. M. *Inorg. Chim. Acta* **1991**, *185*, 143–154. (b) Manojlovic-Muir, L.; Muir, K. W.; Solomun, T. *J. Organomet. Chem.* **1977**, *142*, 265–280. (c) Kapoor, P.; Loevqvist, K.; Oskarsson, Å. *J. Mol. Struct.* **1998**, *470*, 39–47.
(6) Some examples: (a) Michelin, R. A.; Ros, R. *J. Chem. Soc., Dalton Trans.* **1989**, 1149–1159. (b) Otto, S.; Roodt, A. *Inorg. Chim. Acta* **2004**, *357*, 1–10. (c) Roodt, A.; Otto, S.; Steyl, G. *Coord. Chem. Rev.* **2003**, *245*, 121–137. (d) Honeychuck, R. V.; Hersh, W. H. *Inorg. Chem.* **1987**, *26*, 1826–1828. (e) Arnold, D. P.; Bennett, M. A. *Inorg. Chem.* **1984**, *23*, 2117–2124. (f) Cairns, M. A.; Dixon, K. R.; Rivett, G. A. *J. Organomet. Chem.* **1979**, *171*, 373–385. (g) Church, M. J.; Mays, M. J. *J. Chem. Soc.* (*A*) **1970**, 1938–1941. (h) Appleton, T. G.; Hall, J. R.; Ralph, S. F. *Inorg. Chem.* **1985**, *24*, 4685–4693.
(7) For instance: (a) Steyn, G. J. J.; Roodt, A.; Poletaeva, I.; Varshavsky, Yu. S. *J. Organomet. Chem.* **1997**, *536−537*, 197–205. (b) Mather, G. G.; Pidcock, A.; Rapsey, G. J. N. *J. Chem. Soc., Dalton Trans.* **1973**, 2095–2099. (c) Otto, S.; Roodt, A.; Leipoldt, J. G. *S. Afr. J. Chem.* **1995**, *48*, 114–119.

Scheme 1

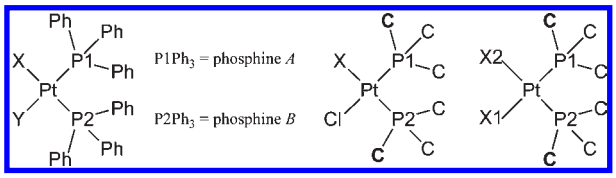

which can be considered an estimate of the bond strength between these atoms. Correlations between the two studies have also been reported.[7]

In a previous paper,[8] we have used the $^1J_{PtP}$ coupling constants of a series of *trans*-$[PtX_2(PPh_3)_2]$ and *trans*-$[PtXY(PPh_3)_2]$ complexes to investigate the cis influence of some anionic ligands X and Y. We assumed that in these complexes the mutual trans influence of the two phosphines can be considered constant to a good approximation and that the $^1J_{PtP}$ values of the various complexes should depend, essentially, on the cis influence of X and/or Y. The series of cis influence obtained was the following:[8]

$$I > Cl > SePh \cong SPh \cong SeEt > NO_3 > AcO > NO_2 > H > Me > Ph$$

When we moved to the *cis*-$[PtXY(PPh_3)_2]$ derivatives, we reasoned that the Pt−P bond strengths must depend on both trans and cis influences. For instance, $^1J_{PtP1}$ (see Scheme 1) should depend not only on the trans influence of Y, but also on the cis influence of X. The latter has been little studied, and although its contribution is usually believed to be of lower importance,[4,9,10] we wondered whether it could be observed, evaluated, and compared with the trans influence. This paper tries and addresses these points. We will discriminate the two contributions analyzing (i) the Pt−P bond distances of the seven X-ray crystal structures we have determined, together with some literature data, (ii) the Pt−P bond distances of the optimized geometries of some derivatives, and (iii) the one bond coupling constants of several compounds. We will also compare the different magnitudes of the cis and trans influences. The nomenclature used in this paper is summarized in Scheme 1.

Experimental Section

General. Chemicals were reagent grade and used as received. Elemental analyses were performed at the Microanalytical Laboratory of the Università degli Studi di Milano. $^{31}P\{^1H\}$ NMR spectra were recorded in $CDCl_3$ on a Bruker Advance DRX 300 at 121 MHz; δ_P values (ppm) are versus external H_3PO_4, *J* coupling constants (Hz) have been found reproducible to ±3 Hz. Electrospray ionization (ESI) mass spectra were recorded with a LCQ Advantage Thermofluxional Instrument. Infrared spectra were recorded as KBr disks using a JASCO FT-IR 410 spectrophotometer with a 2 cm^{-1} resolution, and main bands are given in inverse centimeters. *cis*-$[PtCl_2(PPh_3)_2]$ (**1**),[11] *cis*-$[Pt(AcO)_2(PPh_3)_2]$ (**3**),[12] and *cis*-$[Pt(NO_3)_2(PPh_3)_2]$ (**5**)[12] were synthesized as described in the literature. Crystals of **3** suitable for X-ray diffraction were obtained by slow evaporation of a diisopropyl ether/chloroform solution, whereas crystals of **5** suitable for X-ray diffraction were obtained by slow diffusion of diisopropyl ether into a chloroform or a dichloromethane solution. *All reactions involving silver salts were performed in the dark.*

Synthetic Procedures: *cis*-$[PtCl(AcO)(PPh_3)_2]$ (2). AgAcO (21.1 mg, 0.13 mmol) was added to a solution of **1** (100.1 mg, 0.13 mmol) in CH_2Cl_2 (10 mL). The mixture was refluxed for 8 h, hot filtered, and the filtrate was evaporated to dryness in vacuo yielding **2** as a white solid (74.2 mg, 70%). Anal. calcd for $C_{38}H_{33}ClO_2P_2Pt \cdot CH_2Cl_2$ (899.09): C, 52.10; H, 3.92. Found: C, 52.51; H, 4.09. IR (KBr): 1628, 1370, and 1311 (ν_{CO}). δ_P 3.1 (1P, d, J_{PP} 19, J_{PtP} 3560), 18.3 (1P, d, J_{PP} 19, J_{PtP} 3956). ESI-MS: *m*/*z* 719 ($[Pt(PPh_3)_2]^+$, 100%), 754 ($[PtCl(PPh_3)_2]^+$, 60), 778 ($[Pt(AcO)(PPh_3)_2]^+$, 65), 836 ($[M + Na]^+$, 25). Crystals suitable for X-ray diffraction were obtained by slow diffusion of diisopropyl ether into a chloroform solution.

***cis*-$[PtCl(NO_3)(PPh_3)_2]$ (4).** $AgNO_3$ (21.8 mg, 0.13 mmol) was added to a solution of **1** (94.6 mg, 0.12 mmol) in CH_2Cl_2 (10 mL). The mixture was refluxed for 8 h, hot filtered, and the filtrate was taken to dryness yielding **4** as a white solid (40.1 mg, 41%). Anal. calcd for $C_{36}H_{30}NClO_3P_2Pt \cdot CH_2Cl_2$ (902.05): C, 49.27; H, 3.58; N, 1.55. Found: C, 49.60; H, 3.61; N, 1.55. IR (KBr): 1499 and 1273 (ν_{NO3}). δ_P 2.7 (1P, d, J_{PP} 19, J_{PtP} 3858), 17.6 (1P, d, J_{PP} 19, J_{PtP} 3842). Crystals suitable for X-ray diffraction were obtained by slow diffusion of diisopropyl ether into a chloroform solution.

Observed Formation of *cis*-$[PtBrCl(PPh_3)_2]$ (6). Solid KBr (174.8 mg, 1.47 mmol) was added to a solution of K_2PtCl_4 (152.4 mg, 0.37 mmol) in water (5 mL). This solution was added to a solution of PPh_3 (192.6 mg, 0.73 mmol) in ethanol (15 mL), and the mixture was stirred at room temperature for 4 h, when a very light yellow solid was recovered by filtration. Its ^{31}P NMR spectrum showed the presence of *cis*-$[PtCl_2(PPh_3)_2]$ (**1**), *cis*-$[PtBr_2(PPh_3)_2]$ (**7**), and a new series of signals, δ_P 13.6 (d, J_{PP} 14, J_{PtP} 3665), 15.3 (d, J_{PP} 14, J_{PtP} 3618), assigned to **6**, in a 1:1:2 ratio (see the Results and Discussion section).

***cis*-$[PtBr_2(PPh_3)_2]$ (7).** Solid KBr (411.7 mg, 3.46 mmol) was added to a solution of K_2PtCl_4 (199.8 mg, 0.48 mmol) in water (7 mL). The resulting solution was added to a solution of PPh_3 (258.2 mg, 0.98 mmol) in ethanol (15 mL), and the mixture was refluxed for 4 h. The very light yellow product was recovered by filtration of the cooled mixture (380.1 mg, 90%). Anal. calcd for $C_{36}H_{30}Br_2P_2Pt$ (879.47): C, 49.17; H, 3.44. Found: C, 49.40; H, 3.51. δ_P 14.3 (2P, s, J_{PtP} 3614). ESI-MS: *m*/*z* 719 ($[Pt(PPh_3)_2]^+$, 80%), 799 ($[PtBr(PPh_3)_2]^+$, 100), 902 ($[M + Na]^+$, 10). Crystals suitable for X-ray diffraction were obtained by slow diffusion of diisopropyl ether into a chloroform/dichloromethane solution.

***cis*-$[PtBr(AcO)(PPh_3)_2]$ (8).** AgAcO (15.8 mg, 0.095 mmol) was added to a solution of **7** (80.3 mg, 0.091 mmol) in CH_2Cl_2 (10 mL). The mixture was stirred at room temperature for 8 h, filtered hot, and the filtrate was concentrated and precipitated with diisopropyl ether, yielding a very light yellow solid (65.5 mg, 80%). Anal. calcd for $C_{38}H_{33}BrO_2P_2Pt \cdot 2H_2O$ (894.64): C, 51.02; H, 4.25. Found: C, 51.03; H, 3.95. ESI-HRMS: *m*/*z* Calcd for $[M + Na]^+$: 881.06748. Found: 881.06687. δ_P 2.0 (1P, d, J_{PP} 17, J_{PtP} 3538), 18.8 (1P, d, J_{PP} 17, J_{PtP} 3907).

***cis*-$[PtBr(NO_3)(PPh_3)_2]$ (9).** $AgNO_3$ (22.1 mg, 0.13 mmol) was added to a solution of **7** (111.0 mg, 0.13 mmol) in CH_2Cl_2 (15 mL). The mixture was refluxed for 4 h, filtered hot, and the filtrate was concentrated and precipitated with diisopropyl ether, yielding a very light yellow solid. The crude product was recrystallized from CH_2Cl_2−*n*-hexane (30.1 mg, 27%). Anal. calcd for $C_{36}H_{30}BrNO_3P_2Pt$ (861.568): C, 50.19; H, 3.51; N, 1.63. Found: C, 50.34; H, 3.48; N, 1.76. δ_P 1.5 (1P, d, J_{PP} 17, J_{PtP} 3826), 17.8 (1P, d, J_{PP} 17, J_{PtP} 3790).

***cis*-$[PtClI(PPh_3)_2]$ (10).** A solution of KI (672.2 mg, 4.48 mmol) in H_2O (5 mL) and EtOH (5 mL) was added to a white suspension of **1** (86.5 mg, 0.11 mmol) in $CHCl_3$ (5 mL) and

(8) Rigamonti, L.; Manassero, C.; Rusconi, M.; Manassero, M.; Pasini, A. *Dalton Trans.* **2009**, 1206–1213.
(9) Muenzenberg, R.; Rademacher, P.; Boese, R. *J. Mol. Struct.* **1998**, *444*, 77–90.
(10) Tau, K. D.; Meek, D. W. *Inorg. Chem.* **1979**, *18*, 3574–3580.
(11) Hartley, F. R. *Organomet. Chem. Rev. A* **1970**, *6*, 119–137.
(12) Alesi, M.; Fantasia, S.; Manassero, M.; Pasini, A. *Eur. J. Inorg. Chem.* **2006**, 1429–1435.

acetone (5 mL). The yellow mixture was left under reflux for 1 h, and then the yellow solid was filtered, washed with H_2O, EtOH, and diisopropyl ether, and dried. The crude product was recrystallized from CH_2Cl_2−diisopropyl ether, yielding **10** as light yellow polycrystalline solid (42.1 mg, 43%). Anal. calcd for $C_{36}H_{30}ClIP_2Pt$ (882.02): C, 49.02; H, 3.43. Found: C, 49.29; H, 3.32. δ_P 11.6 (1P, d, J_{PP} 12, J_{PtP} 3683), 13.7 (1P, d, J_{PP} 12, J_{PtP} 3420).

[PtI$_2$(cod)]. Solid KI (833.7 mg, 5.02 mmol) was added to a solution of K_2PtCl_4 (327.6 mg, 0.79 mmol) in water (10 mL). After 10 min, acetic acid (10 mL) and cod (390 μL, 3.17 mmol) were added to the dark solution. The mixture was left at 80 °C for 2 h. After cooling, the product was recovered as a yellow solid by filtration, washed with water, ethanol, and diisopropyl ether, and dried in vacuo (395.2 mg, 90%). Anal. calcd for $C_8H_{12}I_2Pt$ (557.07): C, 17.25; H, 2.17. Found: C, 17.40; H, 2.36. IR (KBr): 1499, 1422, and 1340 (ν_{CC}).

***cis*-[PtI$_2$(PPh$_3$)$_2$] (11).** A solution of PPh_3 (107.8 mg, 0.41 mmol) in CH_2Cl_2 (5 mL) was added dropwise to a solution of [PtI$_2$(cod)] (119.6 mg, 0.21 mmol) in CH_2Cl_2 (5 mL) and the mixture was stirred at room temperature for 5 min. The resulting pale yellow solid was filtered, washed with CH_2Cl_2 and diisopropyl ether, and dried in vacuo (183.9 mg, 87%). Anal. calcd for $C_{36}H_{30}I_2P_2Pt\cdot 3H_2O$ (1027.51): C, 42.08; H, 3.53. Found: C, 42.11; H, 3.63. ^{31}P NMR showed that this solid consisted of a 1:2 mixture of the cis and trans isomers: δ_P 12.6 (s, J_{PtP} 2493) *trans*-[PtI$_2$(PPh$_3$)$_2$], 11.9 (s, J_{PtP} 3455) *cis*-[PtI$_2$(PPh$_3$)$_2$] (**11**). Refluxing this mixture in ethanol (15 mL) in the presence of an excess of PPh_3 gave complete isomerization to *trans*-[PtI$_2$(PPh$_3$)$_2$] (NMR evidence). Slow crystallization from chloroform−diisopropyl ether gave deep orange and yellow crystals. The former consisted of *trans*-[PtI$_2$(PPh$_3$)$_2$], whose structure is already published.[13] The yellow crystals were found to be suitable for X-ray crystallography and consisted of **11**.

***cis*-[PtI(NO$_3$)(PPh$_3$)$_2$] (12).** KI (13.3 mg, 0.080 mmol) was added to a solution of **5** (130.3 mg, 0.15 mmol) in CH_2Cl_2 (5 mL) and $CHCl_3$ (5 mL). The mixture was refluxed for 4 h and then filtered hot. The filtrate was taken to dryness yielding a yellow−orange solid. The crude product was recrystallized twice from dichloromethane−diisopropyl ether, yielding **12** as a yellow powder (45.6 mg, 30%). Anal. calcd for $C_{36}H_{30}INO_3P_2Pt\cdot CHCl_3$ (1027.95): C, 43.23; H, 3.04; N, 1.36. Found: C, 42.98; H, 3.33; N, 1.32. IR (KBr): 1497 and 1272 (ν_{NO3}). δ_P −0.5 (1P, d, J_{PP} 14, J_{PtP} 3819), 15.5 (1P, d, J_{PP} 14, J_{PtP} 3596).

***cis*-[PtCl(NO$_2$)(PPh$_3$)$_2$] (13).** $AgNO_2$ (87.8 mg, 0.57 mmol) was added to a solution of **1** (100.3 mg, 0.13 mmol) in $CHCl_3$:CH_2Cl_2 1:1 (10 mL). The mixture was refluxed for 3 days, hot filtered, and the filtrate was evaporated to dryness yielding **13** as a white solid (105.2 mg, 99%). Anal. calcd for $C_{36}H_{30}NClO_2P_2Pt$ (801.12): C, 53.97; H, 3.77; N, 1.75. Found: C, 53.56; H, 4.42; N, 1.86. IR (KBr): 1410 and 1335 (ν_{NO2}). δ_P −0.5 (1P, d, J_{PP} 20, J_{PtP} 2883), 12.2 (1P, d, J_{PP} 20, J_{PtP} 3949). ESI-MS: m/z 719 ([Pt(PPh$_3$)$_2$]$^+$, 50%), 754 ([PtCl(PPh$_3$)$_2$]$^+$, 100), 765 ([Pt(NO$_2$)(PPh$_3$)$_2$]$^+$, 90), 824 ([M + Na]$^+$, 15), 1625 ([2 M + Na]$^+$, 50). Crystals suitable for X-ray diffraction were obtained by slow diffusion of diisopropyl ether into a chloroform solution.

***cis*-[Pt(NO$_2$)$_2$(PPh$_3$)$_2$] (14).** The reaction was performed under an argon atmosphere in a Schlenk tube. Solid $AgNO_2$ (230.8 mg, 1.50 mmol) was added to a solution of **1** (94.5 mg, 0.12 mmol) in dried $CHCl_3$ (7 mL), and the mixture was left under reflux for 15 h. The mixture was filtered hot and the filtrate was taken almost to dryness, yielding a very light yellow solid, filtrated and washed with diisopropyl ether (85.6 mg, 88%). Anal. calcd for $C_{36}H_{30}N_2O_4P_2Pt$ (811.67): C, 53.27; H, 3.73; N, 3.45. Found: C, 53.36; H, 3.65; N, 3.56. IR (KBr): 1412 and 1336 (ν_{NO2}). δ_P −1.3 (2P, s, J_{PtP} 3148).

X-ray Data Collections and Structure Determinations. Crystal data are summarized in Table 1. The diffraction experiments were carried out on a Bruker APEX II CCD area-detector diffractometer, at 150 K for **7** and **13**, and at 296 K for **2**, **3**·0.25H$_2$O, **4**·CHCl$_3$, **5**·CH$_2$Cl$_2$, **5**·CHCl$_3$, and **11**·H$_2$O, using Mo Kα radiation (λ = 0.71073 Å) with a graphite crystal monochromator in the incident beam. No crystal decay was observed, so that no time-decay correction was needed. The collected frames were processed with the software SAINT,[14] and an empirical absorption correction was applied (SADABS)[15] to the collected reflections. The calculations were performed using the Personal Structure Determination Package[16] and the physical constants tabulated therein.[17] The structures were solved by direct methods (SHELXS)[18] and refined by full-matrix least-squares using all reflections and minimizing the function $\Sigma w(F_o^2 - kF_c^2)^2$ (refinement on F^2). In **4**·CHCl$_3$, the solvent molecule is disordered: the carbon atom (C1) and the first Cl atom (Cl2) are ordered, whereas the second Cl atom is split into two peaks (Cl3 and Cl4) having occupancies of 0.50 each, and the third Cl atom is split into four peaks (Cl5, Cl6, Cl7, and Cl8) having occupancies of 0.25 each. In spite of this, all the non-hydrogen atoms of this molecule could be refined with anisotropic thermal factors, whereas the hydrogen atom was obviously ignored. In **3**·0.25H$_2$O, the water oxygen atom has an occupancy factor of 0.50 but could be refined with an anisotropic thermal factor. Surprisingly, its two hydrogen atoms were detected in the final Fourier maps and included in the structure factor calculations with occupancies 0.50 each, and not refined. In **11**·H$_2$O, the oxygen atom of the solvent molecule has an occupancy factor of 1.00, but its hydrogen atoms were not detected in the final Fourier maps and were ignored. In **5**·CH$_2$Cl$_2$ and **5**·CHCl$_3$, the solvent molecules are ordered and were treated normally. In **2** and **3**·0.25H$_2$O, the hydrogen atoms of the CH$_3$ groups belonging to the acetato ligands were detected in the final Fourier maps and not refined. All the other hydrogen atoms were placed in their ideal positions (C−H = 0.97 Å), with the thermal parameter U being 1.10 times that of the atom to which they are attached, and not refined. All the non-hydrogen atoms of the eight compounds were refined with anisotropic thermal parameters. For chiral **2**, full refinement of the correct structure enantiomorph led to $R_2 = 0.028$ and $R_{2w} = 0.043$, full refinement of the wrong one led to $R_2 = 0.096$ and $R_{2w} = 0.163$. For chiral **3**·0.25H$_2$O, full refinement of the correct

(13) Boag, N. M.; Mohan Rao, K.; Terrill, N. J. *Acta Cryst. Sect. C* **1991**, *C47*, 1064–1065.

(14) *SAINT Reference manual*; Siemens Energy and Automation: Madison, W1, 1994−1996.

(15) Sheldrick, G. M. *SADABS, Empirical Absorption Correction Program*; University of Göttingen, Göttingen, Germany, 1997.

(16) Frenz, B. A. *Comput. Phys.* **1988**, *2*, 42–48.

(17) *Crystallographic Computing 5*; Oxford University Press: Oxford, U.K., 1991; Chapter 11, p 126.

(18) Sheldrick, G. M. *SHELXS 86. Program for the solution of crystal structures*; University of Göttingen, Göttingen, Germany, 1985.

(19) Frisch, M. J.; Trucks, G. W.; Schlegel, H. B.; Scuseria, G. E.; Robb, M. A.; Cheeseman, J. R.; Montgomery, J. A., Jr.; Vreven, T.; Kudin, K. N.; Burant, J. C.; Millam, J. M.; Iyengar, S. S.; Tomasi, J.; Barone, V.; Mennucci, B.; Cossi, M.; Scalmani, G.; Rega, N.; Petersson, G. A.; Nakatsuji, H.; Hada, M.; Ehara, M.; Toyota, K.; Fukuda, R.; Hasegawa, J.; Ishida, M.; Nakajima, T.; Honda, Y.; Kitao, O.; Nakai, H.; Klene, M.; Li, X.; Knox, J. E.; Hratchian, H. P.; Cross, J. B.; Adamo, C.; Jaramillo, J.; Gomperts, R.; Stratmann, R. E.; Yazyev, O.; Austin, A. J.; Cammi, R.; Pomelli, C.; Ochterski, J. W.; Ayala, P. Y.; Morokuma, K.; Voth, G. A.; Salvador, P.; Dannenberg, J. J.; Zakrzewski, V. G.; Dapprich, S.; Daniels, A. D.; Strain, M. C.; Farkas, O.; Malick, D. K.; Rabuck, A. D.; Raghavachari, K.; Foresman, J. B.; Ortiz, J. V.; Cui, Q.; Baboul, A. G.; Clifford, S.; Cioslowski, J.; Stefanov, B. B.; Liu, G.; Liashenko, A.; Piskorz, P.; Komaromi, I.; Martin, R. L.; Fox, D. J.; Keith, T.; Al-Laham, M. A.; Peng, C. Y.; Nanayakkara, A.; Challacombe, M.; Gill, P. M. W.; Johnson, B.; Chen, W.; Wong, M. W.; Gonzalez, C.; Pople, J. A. *Gaussian 03*, revision B.04; Gaussian, Inc.: Pittsburgh, PA, 2003.

Table 1. Crystallographic Data

compound	**2**	**3**·0.25H_2O	**4**·$CHCl_3$	**5**·CH_2Cl_2
formula	$C_{38}H_{33}ClO_2P_2Pt$	$C_{160}H_{146}O_{17}P_8Pt_4$	$C_{37}H_{31}Cl_4NO_3P_2Pt$	$C_{37}H_{32}Cl_2N_2O_6P_2Pt$
M	814.18	3369.09	936.51	928.62
crystal system	orthorhombic	orthorhombic	triclinic	monoclinic
space group	$P2_12_12_1$	$P2_12_12_1$	$P\bar{1}$	$P2_1/n$
a/Å	10.1657(6)	10.4372(7)	11.1572(5)	11.9715(7)
b/Å	17.6477(10)	18.6546(12)	11.6921(5)	20.0334(11)
c/Å	18.5574(10)	34.9948(22)	14.6755(7)	15.4580(9)
α/deg	90	90	92.144(1)	90
β/deg	90	90	96.166(1)	95.190(1)
γ/deg	90	90	106.110(1)	90
U/Å^3	3329.2(3)	6813.6(9)	1824.1(1)	3692.1(4)
Z	4	2	2	4
F(000)	1608	3348	920	1832
D_c/g·cm^{-3}	1.624	1.642	1.705	1.671
crystal dimensions/mm	0.25 × 0.35 × 0.45	0.05 × 0.45 × 0.50	0.12 × 0.20 × 0.25	0.32 × 0.34 × 0.37
μ (Mo Kα)/cm^{-1}	44.65	42.94	43.04	41.16
minimum and maximum transmission factors	0.677−1.000	0.556−1.000	0.594−1.000	0.822−1.000
T/K	296	296	296	296
λ (Mo Kα)	0.71073	0.71073	0.71073	0.71073
scan mode	ω	ω	ω	ω
frame width/deg	0.50	0.50	0.50	0.50
time per frame/s	15	10	20	20
no. of frames	3960	2580	3013	3300
detector−sample distance/cm	6.00	6.50	5.00	6.00
θ range	3.00−29.00	3.00−28.00	3.00−29.00	3.00−28.00
reciprocal space explored	full sphere	full sphere	full sphere	full sphere
no. of reflections (total; independent)	112229; 8960	131789; 16557	60430; 11538	104889; 9948
R_{int}	0.0286	0.0508	0.0246	0.0296
final R_2 and R_{2w} indices[a] (F^2, all reflections)	0.028, 0.043	0.044, 0.063	0.031, 0.048	0.031, 0.047
conventional R_1 index ($I > \sigma(I)$)	0.017	0.028	0.022	0.020
reflections with $I > 2\sigma(I)$	8500	15201	9926	7911
no. of variables	397	856	469	451
goodness of fit[b]	0.988	1.007	1.012	1.039

Compound	**5**·$CHCl_3$	**7**	**11**·H_2O	**13**
formula	$C_{37}H_{31}Cl_3N_2O_6P_2Pt$	$C_{36}H_{30}Br_2P_2Pt$	$C_{36}H_{30}I_2OP_2Pt$	$C_{36}H_{30}ClNO_2P_2Pt$
M	963.07	879.50	989.49	801.14
crystal system	monoclinic	monoclinic	triclinic	monoclinic
space group	$P2_1/n$	$P2_1/c$	$P\bar{1}$	$P2_1/c$
a/Å	12.0353(6)	32.6290(21)	9.8799(5)	9.5838(2)
b/Å	19.9799(10)	9.6539(6)	10.5936(6)	17.2369(3)
c/Å	15.8339(8)	19.8452(13)	17.8664(9)	19.3496(3)
α/deg	90	90	86.690(1)	90
β/deg	95.330(1)	93.810(1)	78.110(1)	99.869(1)
γ/deg	90	90	69.880(1)	90
U/Å^3	3791.0(3)	6237.4(8)	1718.0(2)	3149.2(1)
Z	4	8	2	4
F(000)	1896	3392	936	1576
D_c/g·cm^{-3}	1.687	1.873	1.913	1.690
crystal dimensions/mm	0.03 × 0.03 × 0.25	0.08 × 0.35 × 0.45	0.20 × 0.25 × 0.45	0.21 × 0.23 × 0.48
μ (Mo Kα)/cm^{-1}	40.81	72.10	60.22	47.20
minimum and maximum transmission factors	0.571−1.000	0.275−1.000	0.496−1.000	0.499−1.000
T/K	296	150	296	150
λ (Mo Kα)	0.71073	0.71073	0.71073	0.71073
scan mode	ω	ω	ω	ω
frame width/deg	0.50	0.50	0.50	0.40
time per frame/s	30	20	20	10
no. of frames	2220	2880	2400	1320
detector−sample distance/cm	5.00	6.00	5.00	6.00
θ range	3.00 − 29.00	3.00 − 26.00	3.00 − 29.00	3.00 − 26.00
reciprocal space explored	full sphere	full sphere	full sphere	full sphere
no. of reflections (total; independent)	99490; 13130	113116; 13475	48198; 11669	25153; 7362
R_{int}	0.0719	0.0567	0.0286	0.0550
final R_2 and R_{2w} indices[a] (F^2, all reflections)	0.050, 0.057	0.069, 0.116	0.059, 0.096	0.063, 0.086
conventional R_1 index ($I > \sigma(I)$)	0.034	0.048	0.034	0.038
reflections with $I > 2\sigma(I)$	8373	8896	7302	4577
no. of variables	460	740	370	388
goodness of fit[b]	0.976	1.002	0.986	0.974

[a] $R_2 = [\Sigma(|F_o^2 - kF_c^2|/\Sigma F_o^2]$, $R_{2w} = [\Sigma w(F_o^2 - kF_c^2)^2/\Sigma w(F_o^2)^2]^{1/2}$. [b] $[\Sigma w(F_o^2 - kF_c^2)^2/(N_o - N_v)]^{1/2}$, where $w = 4F_o^2/\sigma(F_o^2)^2$, $\sigma(F_o^2) = [\sigma^2(F_o^2) + (pF_o^2)^2]^{1/2}$, N_o is the number of observations, N_v is the number of variables, $p = 0.02$ for **4**·$CHCl_3$, **5**·CH_2Cl_2, **5**·$CHCl_3$, and **11**·H_2O, and $p = 0.03$ for **2**, **3**·0.25H_2O, **7**, and **13**.

structure enantiomorph led to $R_2 = 0.044$ and $R_{2w} = 0.063$, full refinement of the wrong one led to $R_2 = 0.096$ and $R_{2w} = 0.153$. In the final Fourier maps, the maximum residuals were 1.94(13) e·Å^{-3} at 0.73 Å from Pt, 3.01(26) e·Å^{-3} at 0.83 Å from Pt, 1.71(18) e·Å^{-3} at 0.63 Å from Pt, 1.18(20) e·Å^{-3} at 0.08 Å from Cl2, 1.44(44) e·Å^{-3} at 1.03 Å from P1, 2.63(78) e·Å^{-3} at 0.62 Å from Pt, 2.42(73) e·Å^{-3} at 0.55 Å from Pt, and 2.41(50) e·Å^{-3} at 0.78 Å from Pt, for **2**, **3**·0.25H_2O, **4**·$CHCl_3$, **5**·CH_2Cl_2, 5·$CHCl_3$, **7**, **11**·H_2O, and **13**, respectively. Minimum peaks (holes), in the same order, were −1.00(13), −2.63(26), −1.33(18), −0.96(20), −1.28(44), −3.35(78), −2.35(73), and −1.94(50) e·Å^{-3}, respectively. CCDC 741800−741807 contain the supplementary crystallographic data for this paper.

Computational Details. Calculations were performed with the Gaussian 03 program package.[19] All geometries were fully optimized using the B3LYP functional[20] and the def2-SVP split valence basis set with polarization functions on all atoms.[21,22] In particular, an extra set of *f* functions with exponent 0.66813 has been used for Pt. I and Pt have been treated as a 25- and an 18-electron system, respectively, with relativistic effective core potentials (ECP's) taken from the literature.[23,24] The natural bond orbital (NBO) analysis[25] was used for evaluating the *s* character of the hybrid orbitals involved in the Pt−P bonds in the different complexes.

Results and Discussion

Preparation and Characterization. The majority of the compounds were prepared by metathesis reaction, treating *cis*-[$PtCl_2(PPh_3)_2$] (**1**) with the appropriate silver or potassium salt. *cis*-[$PtI_2(PPh_3)_2$] (**11**) was prepared by reaction of [PtI_2(cod)] (cod = cyclooctadiene) with PPh_3. This reaction, however, gave a mixture of cis/trans derivatives. Also the reported preparation of **11** by treatment of **1** with NaI[26] gave, in our hands, a substantial amount of the trans isomer. Pure samples of the cis isomer were obtained by careful crystallization of these mixtures. Interestingly, refluxing an ethanol suspension of these mixtures with excess PPh_3 gave pure *trans*-[$PtI_2(PPh_3)_2$], in contrast with the behavior of the cis/trans dichloro complexes, for which a similar treatment gives rise to complete isomerization to **1**.[27]

The synthesis of *cis*-[$PtBr_2(PPh_3)_2$] (**7**) was carried out following the same synthetic procedure of **1**,[11] from $K_2[PtBr_4]$, prepared in situ by the addition of a large excess of KBr added to $K_2[PtCl_4]$. If the synthesis of **7** was performed using lower amounts of KBr, we detected an intermediate. Under these conditions, the ^{31}P NMR spectra of the crude products showed the presence of the singlets of **1** and **7** and two doublets of the new compound. The concentrations of **1** and the latter diminished, increasing the amount of KBr, and eventually disappeared when a large excess was used, giving **7** analytically pure. We interpreted these facts as the observation of the stepwise substitution of Cl by Br, and consequently assigned the two doublets to *cis*-[$PtBrCl(PPh_3)_2$] (**6**) unambiguously. Attempts to isolate it failed, because of the very similar solubility of **1**, **6**, and **7** (in the Experimental Section we reported the conditions which give the highest concentration of **6** in the mixture). *cis*-[$PtBr(NO_3)(PPh_3)_2$] (**9**), *cis*-[$PtClI(PPh_3)_2$] (**10**) and *cis*-[$PtI(NO_3)(PPh_3)_2$] (**12**) were obtained pure only after careful recrystallization, but in rather low yields. The synthesis of *cis*-[$Pt(NO_2)_2(PPh_3)_2$] (**14**) was found to be rather "tricky", since this compound was often impure of the oxidation product *cis*-[$Pt(NO_3)_2(PPh_3)_2$] (**5**); only performing the reaction under a strict argon atmosphere we managed to obtain **14** analytically pure.

The cis configuration of compounds **2**, **3**, **4**, **5**, **7**, **11**, and **13** was unambiguously assigned by X-ray structural determinations (see below). The cis geometry of the mixed *cis*-[$PtXY(PPh_3)_2$] complexes was confirmed by the presence, in their ^{31}P NMR spectra, of two doublets, due to the nonequivalent P atoms. An IR criterion[8,26,28] was also used: an intense band at around 550 cm^{-1}, probably a PC_3 overtone, has been reported to be typical of *cis*-$Pt(PPh_3)_2$ complexes, it being absent, or very weak, in the trans derivatives. This criterion was found to hold each time we could compare it with X-ray structures or ^{31}P NMR evidence.

X-ray Structures. We have performed the X-ray structural determinations of compounds **2**, **3**·0.25H_2O, **4**·$CHCl_3$, **5**·CH_2Cl_2, **5**·$CHCl_3$, **7**, **11**·H_2O, and **13**. ORTEP views of compounds **3**, **11**, and **13** are presented in Figures 1−3; pictures of the other compounds can be found in the Supporting Information. Relevant bond lengths and angles, together with those of compound **1**,[29] are collected in Tables 2−4.

All complexes present a square planar coordination of the Pt atom, with minor distortions. In **3** the two acetato and in **5** the two nitrato groups are almost perpendicular to the coordination plane and in an anticonfiguration with respect to it, giving rise to chirality.[30] In **3**·0.25H_2O the elementary cell contains both enantiomeric arrangements.

Bond lengths and angles are within the normal ranges, the Pt−P bonds are shorter while the Pt−Cl and Pt−O (acetato and nitrato) are longer than those found in the corresponding trans isomers.[8,13,31,32]

A careful inspection of the structures reveals an interesting feature that to our knowledge has never been described previously. In fact there is a relationship

(20) (a) Lee, C. T.; Yang, W. T.; Parr, R. G. *Phys. Rev. B* **1988**, *37*, 785–789. (b) Becke, A. D. *J. Chem. Phys.* **1993**, *98*, 5648–5652.
(21) Weigend, F.; Ahlrichs, R. *Phys. Chem. Chem. Phys.* **2005**, *7*, 3297–3305.
(22) (a) Feller, D. *J. Comput. Chem.* **1996**, *17*, 1571–1586. (b) Schuchardt, K. L.; Didier, B. T.; Elsethagen, T.; Sun, L.; Gurumoorthi, V.; Chase, J.; Li, J.; Windus, T. L. *J. Chem. Inf. Model.* **2007**, *47*, 1045–1052.
(23) Peterson, K. A.; Figgen, D.; Goll, E.; Stoll, H.; Dolg, M. *J. Chem. Phys.* **2003**, *119*, 11113–11123.
(24) Andrae, D.; Haeussermann, U.; Dolg, M.; Stoll, H.; Preuss, H. *Theor. Chim. Acta* **1990**, *77*, 123–141.
(25) Reed, A. E.; Curtiss, L. A.; Weinhold, F. *Chem. Rev.* **1988**, *88*, 899–926.
(26) Mastin, S. H. *Inorg. Chem.* **1974**, *13*, 1003–1005.
(27) Anderson, G. K.; Cross, R. J. *Chem. Soc. Rev.* **1980**, *9*, 185–215.
(28) (a) Brune, H. A.; Ertl, J.; Grafl, D.; Schmidtberg, G. *Chem. Ber.* **1982**, *115*, 1141–1153. (b) Brune, H. A.; Ertl, J. *Liebigs Ann. Chem.* **1980**, 928–937.
(29) Fun, H.-K.; Chantrapromma, S.; Liu, Y.-C.; Chen, Z.-F.; Liang, H. *Acta Cryst. Sect. E* **2006**, *E62*, m1252–m1254.
(30) For a discussion on the chirality of square planar complexes see, for instance: (a) Gullotti, M.; Pacchioni, G.; Pasini, A.; Ugo, R. *Inorg, Chem.* **1982**, *21*, 2006–2014. (b) Pasini, A.; De Giacomo, L. *Inorg. Chim. Acta* **1996**, *248*, 225–230. (c) Ano, S. O.; Intini, F. P.; Natile, G.; Marzilli, L. G. *Inorg. Chem.* **1999**, *38*, 2989–2999. (d) Chifotides, H. T.; Dunbar, K. R. *Chem. Eur. J.* **2008**, *14*, 9902–9913. (e) Ranaldo, R.; Margiotta, N.; Intini, F. P.; Pacifico, C.; Natile, G. *Inorg. Chem.* **2008**, *47*, 2820–2830.
(31) Basato, M.; Biffis, A.; Martinati, G.; Tubaro, C.; Venzo, A.; Ganis, P.; Benetollo, F. *Inorg. Chim. Acta* **2003**, *355*, 399–403.
(32) Johanson, M. H.; Otto, S. *Acta Cryst. Sect. C* **2000**, *C56*, e12–e15.

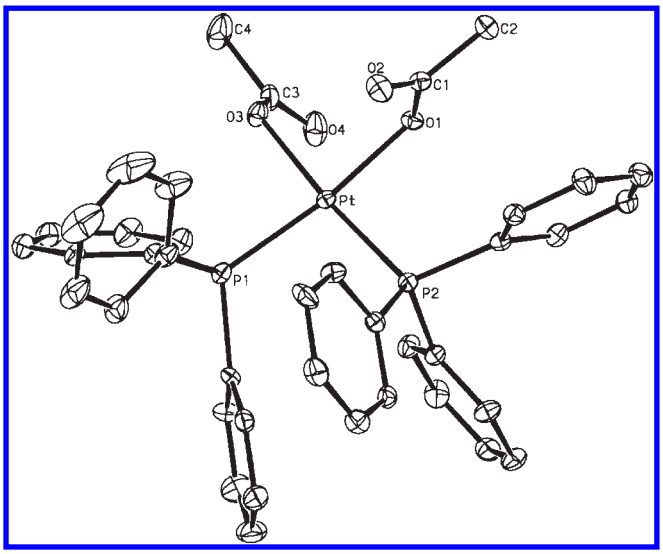

Figure 1. ORTEP view of one independent molecule of *cis*-$[Pt(AcO)_2(PPh_3)_2]$ (**3**·0.25H_2O). Ellipsoids are drawn at the 30% probability; hydrogen atoms and the water molecule are omitted for clarity.

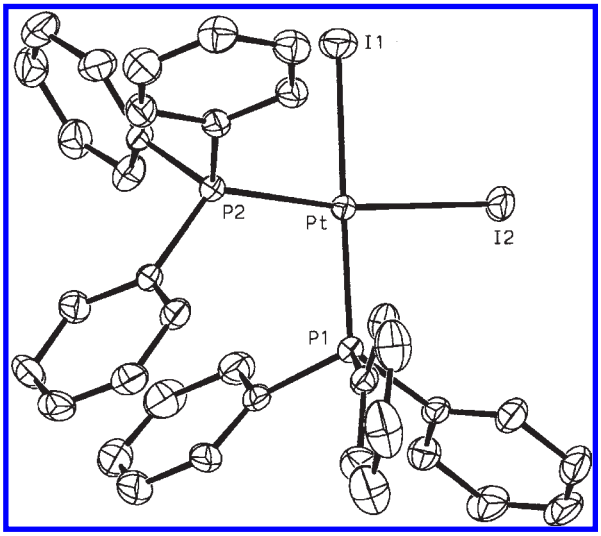

Figure 2. ORTEP view of *cis*-$[PtI_2(PPh_3)_2]$ (**11**·H_2O). Ellipsoids are drawn at the 30% probability; hydrogen atoms and the water molecule are omitted for clarity.

between the conformations of the phosphine groups and Pt−X/Y bond lengths. In the case of the X_2 complexes (with the exception of molecule 2 of **1** and molecule 2 of **7**), the two phosphine groups display different conformations: the ipso carbon atom **C** (in bold in Scheme 1) of phosphine A is almost eclipsed to the X ligand cis to it: the X−Pt−P−C torsion angles vary from 2 to 14° (Tables 2−4); the lowest X−Pt−P−C torsion angles of phosphine B are much larger (34−54°). In the PtX_2 complexes which present this feature, the shorter Pt−P bond is that of phosphine A (i.e., the P atom involved in such eclipsed conformation), while the longer Pt−X bond is trans to such phosphine. In the structures of the three PtClX complexes **2**, **4**, and **13**, phosphine A (the one with the eclipsed **C** atom) is always cis to Y. We think that such adopted molecular conformation allows to optimizing the $\pi-\pi$ interaction between two phenyl rings of the two phosphines.

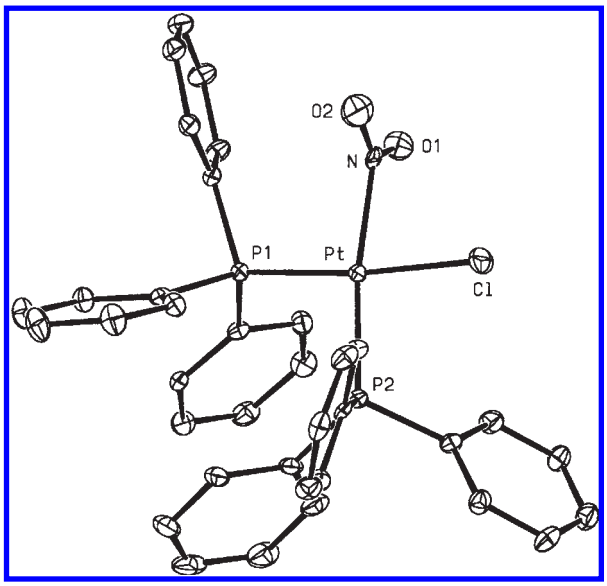

Figure 3. ORTEP view of *cis*-$[PtCl(NO_2)(PPh_3)_2]$ (**13**). Ellipsoids are drawn at the 30% probability; hydrogen atoms are omitted for clarity.

Table 2. Main Distances (Å) and Angles (deg) of the X_2 Compounds **1**, **7**, and **11**·H_2O[a]

	1[b], X = Cl		**7**, X = Br		
	molecule 1	molecule 2	molecule 1	molecule 2	**11**·H_2O, X = I
Pt−P1	2.252(1)	2.271(1)	2.264(2)	2.278(2)	2.277(1)
Pt−P2	2.271(1)	2.261(1)	2.285(2)	2.294(2)	2.292(1)
Pt−X1	2.363(1)	2.351(1)	2.475(1)	2.485(1)	2.656(1)
Pt−X2	2.329(1)	2.348(1)	2.451(1)	2.473(1)	2.634(1)
P1−Pt−P2	99.12(3)	99.93(4)	98.95(6)	99.19(7)	97.83(5)
P2−Pt−X1	83.73(3)	87.35(4)	84.02(5)	86.69(5)	85.17(4)
X2−Pt−P1	89.82(3)	86.25(4)	90.01(5)	87.71(5)	90.64(3)
X1−Pt−X2	87.56(3)	87.73(4)	87.41(3)	87.36(3)	86.78(1)
P1−Pt−X1	175.57(3)	167.58(4)	175.00(5)	171.54(6)	174.87(4)
P2−Pt−X2	170.41(3)	171.13(4)	169.77(5)	169.41(7)	170.06(3)
A[c]	12.6(1)	34.1(1)	14.7(2)	34.1(3)	−14.3(2)
B[d]	−59.5(1)	47.8(1)	60.7(2)	46.7(2)	43.7(2)

[a] P1 trans to X1 for all compounds. [b] Adapted from ref 29. [c] A = lowest X2−Pt−P−**C** torsion angle of phosphine A. [d] B = lowest X1−Pt−P−**C** torsion angle of phosphine B.

Strucural Cis and Trans Influences. In order to study the "structural" cis and trans influences of ligands X and/or Y, we must compare the Pt−P bond distances of the various complexes. To render the discussion easier, this is presented in a table format (Table 5), where we have collected the Pt−P bond distances of the ClX complexes, the Pt−P mean values of the X_2 complexes, and three Pt−P mean values taken from the literature.[29,33,34] Although the individual bond lengths display significant differences, we decided to use the mean values for X_2 derivatives in order to compare these results with the spectroscopic data in solution (one NMR signal); the different bond lengths in the solid state are due to crystal

(33) Yahav, A.; Goldberg, I.; Vigalok, A. *Inorg. Chem.* **2005**, *44*, 1547–1553.
(34) (a) Hannu-Kuure, M. S.; Komulainen, J.; Oilunkaniemi, R.; Laitinen, R. S.; Suontamo, R.; Ahlgrén, M. *J. Organomet. Chem.* **2003**, *666*, 111–120. (b) Hannu, M. S.; Oilunkaniemi, R.; Laitinen, R. S.; Ahlgrén, M. *Inorg. Chem. Commun.* **2000**, *3*, 397–399.

Table 3. Main Distances (Å) and Angles (deg) of the X_2 Compounds **3**·0.25H_2O, **5**·CH_2Cl_2, and **5**·$CHCl_3$[a]

	3·0.25H_2O, X = AcO		**5**, X = NO_3	
	molecule 1	molecule 2	**5**·CH_2Cl_2	**5**·$CHCl_3$
Pt−P1	2.240(1)	2.233(1)	2.239(1)	2.237(1)
Pt−P2	2.243(1)	2.250(1)	2.244(1)	2.247(1)
Pt−O1	2.070(3)	2.079(3)	2.088(2)	2.092(2)
Pt−O3/O4	2.059(3)	2.050(3)	2.092(2)	2.097(2)
P1−Pt−P2	97.90(4)	96.44(4)	97.33(2)	96.96(2)
P2−Pt−O1	87.41(8)	86.96(8)	86.58(4)	87.41(5)
O3/O4−Pt−P1	89.16(8)	89.48(8)	91.17(5)	91.08(6)
O1−Pt−O3/O4	85.44(11)	87.16(11)	84.96(6)	84.56(7)
P1−Pt−O1	174.07(9)	173.97(9)	174.43(4)	174.65(5)
P2−Pt−O3/O4	172.64(8)	174.08(8)	171.49(5)	171.96(6)
A[b]	7.30(17)	−49.06(16)	4.58(11)	1.37(9)
B[c]	33.41(18)	−49.06(16)	−47.70(9)	−49.76(10)

[a] P1 trans to O1 for all compounds, P2 trans to O3 for **3** and to O4 for **5**. [b] A = lowest O3/O4−Pt−P1−**C** torsion angle of phosphine A. [c] B = lowest O1−Pt−P2−**C** torsion angle of phosphine B.

Table 4. Main Distances (Å) and Angles (deg) of ClX Compounds **2**, **4**·$CHCl_3$, and **13**[a]

	2, X = AcO	**4**·$CHCl_3$, X = NO_3	**13**, X = NO_2
Pt−P1	2.244(1)	2.252(1)	2.260(1)
Pt−P2	2.249(1)	2.243(1)	2.284(1)
Pt−Cl	2.345(1)	2.362(1)	2.335(1)
Pt−O1/N	2.070(2)	2.109(1)	2.110(4)
P1−Pt−P2	98.77(2)	98.78(2)	97.39(5)
P2−Pt−Cl	87.58(2)	87.30(2)	88.77(5)
O1/N−Pt−P1	89.32(5)	89.73(4)	90.28(11)
Cl−Pt−O1/N	84.44(5)	84.28(4)	83.55(11)
P1−Pt−Cl	172.36(2)	173.65(2)	173.83(5)
P2−Pt−O1/N	171.80(5)	171.15(4)	172.12(11)
A[b]	−2.18(18)	−14.89(8)	7.48(21)
B[c]	54.50(9)	−51.54(7)	−42.70(18)

[a] P1 trans to Cl for all compounds; P2 trans to O1 for **2** and **4** and to N for **13**. [b] A = lowest O1/N−Pt−P1−**C** torsion angle of phosphine A. [c] B = lowest Cl−Pt−P2−**C** torsion angle of phosphine B.

packing effects as well as the phoshine conformations, as described above, while in solution a mean distance with a symmetric geometry is expected. Appropriate comments and the deductions drawn from such values are inserted in the table.

To begin with, let us consider only the mean Pt−P bond lengths of the X_2 complexes. Following the usually accepted hypothesis[4,9,10] that the cis influence has a lower relevance, we obtain the "structural" trans influence series PhSe > I > Br > Cl > NO_3 ∼ AcO > F. The trans influence can also be observed, for the few data available, from the Pt−P2 bond distances of the mixed ClX complexes, which decreases in the order **1** > **2** > **4** ∼ **13**, giving another trans influence series Cl > AcO > NO_3 ∼ NO_2. The difference of the position of AcO and NO_3 between the two series demonstrates that the cis contribution cannot be neglected. The cis influence is in fact evident if we look at the Pt−P1 bond lengths of the mixed ClX derivatives, which decrease in the order **1** > **13** > **4** > **2**, giving the cis influence order Cl > NO_2 > NO_3 > AcO.[35]

Optimized Geometries. We have performed gas-phase theoretical calculations on the investigated complexes in order to draw further insight on the structural trans and cis influence series. Selected results of geometry optimization of *cis*-[$PtX_2(PPh_3)_2$] and *cis*-[$PtClX(PPh_3)_2$] complexes by B3LYP/def2-SVP calculations are reported in Tables 6 and 7, respectively. Comparison with the available corresponding experimental results indicates that the adopted method reproduces accurately (within 0.02 Å) the Pt−O distances, in particular for *cis*-[$Pt(NO_3)_2(PPh_3)_2$] (**5**). All other interatomic distances involving Pt are overestimated by 0.02−0.08 Å, a typical lengthening of metal−ligand bonds generally obtained by gradient-corrected density functional theory (DFT) methods.[36] An exception to such lengthening is for *cis*-[$PtCl(NO_2)(PPh_3)_2$] (**13**), in which Pt−P2 is 0.112 Å longer than the experimental value and Pt−N is underestimated by 0.034 Å.

Geometry optimization of the X_2 complexes allows to reproduce the experimental finding concerning the relative orientation of the phenyl rings and the consequent deviation from symmetry of the coordination geometry of the metal atom. In all cases, except for X = Ph, we have obtained molecular conformations where atom X2 is nearly eclipsed to the ipso C atom bonded to P1 (phosphine A of Scheme 1), while X1 forms much larger torsion angles with all the ipso C atoms bonded to P2 of phosphine B (see Table 6, torsions A and B, respectively). In agreement with the experimental structures, the Pt−P1 bonds are systematically shorter than the Pt−P2 bonds. The exception is *cis*-[$Pt(Ph)_2(PPh_3)_2$] (**22**), where interference of the phenyl ligands with the PPh_3 groups stabilizes a conformation in which both Ph ligands are located nearly midway the two positions assumed by the substituents in the other complexes.

By looking at the Pt−P1 (or Pt−P2) distances of X_2 complexes, we see that the structural trans influence series reported above is confirmed by our calculations, with the order Ph > NO_2 > I > Br > Cl > AcO ≥ NO_3.

As for the ClX complexes, optimization has been performed starting from *cis*-[$PtCl_2(PPh_3)_2$] (**1**). Because of the observed nonequivalence of the two Pt−Cl bond distances, we have substituted alternatively the Cl positions with an X group. The conformation with X cis to phosphine A was found more stable by up to 3.9 kcal/mol, and this is in fact the only one observed in the available experimental structures of the mixed complexes.

Examination of Table 7 reveals that in such complexes the Pt−P1 bonds (trans to Cl) are virtually unvaried with respect to the Pt−P1 bond of the Cl_2 complex (2.320 Å), suggesting that the presence of an X ligand cis to P1 has no substantial influence (the exceptions are for X = Ph, and, in much lesser extent, NO_2). The Pt−P2 distances (trans to X) are also almost unchanged with respect to the corresponding Pt−P2 distances in the X_2 complexes, excepted for Ph, highlighting the nonobservable structural cis influence. Then, the order of the structural trans influence obtained for the X_2 complexes is confirmed also

(35) Comparison with the sequences obtained in the previous paper[8] holds only for NO_2 > NO_3 > AcO; the position of Cl changes according to the class of complexes considered, suggesting that the actual influences of a ligand depend on its environment, and this will be discussed later.

(36) Koch, W.; Holthausen, M. C. *A Chemist's Guide to Density Functional Theory*, 2nd ed.; Wiley-VCH: New York, 2000.
(37) De Jong, F.; Bour, J. J.; Schlebos, P. P. J. *Inorg. Chim. Acta* **1988**, *154*, 89–93.

Table 5. Summary of the Pt−P Bond Distances

	compound	Pt–P (Å)	comments and deductions	ref
1	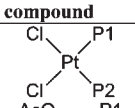	2.264[a]	taken as reference compound	29
2	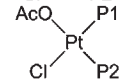	2.244(1) 2.249(1)	Pt–P bonds shorter than in **1**: both *cis* and *trans* influences of AcO lower than Cl	this work
3	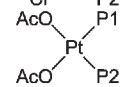	2.242[a]	Pt–P bonds slightly shorter than in **2**, confirming the lower *cis* and *trans* influences of AcO compared to Cl	this work
4	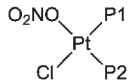	2.252(1) 2.243(1)	Pt–P1 shorter than in **1** but longer than in **2**: *cis* influence of NO_3 lower than Cl, but higher than AcO Pt–P2 shorter than in **1** and similar to **2**: *trans* influences of NO_3 lower than Cl, and similar to AcO	this work
5	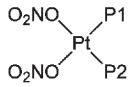	2.242[a]	Pt-P1 shorter than in **4**, confirming that the *trans* influence of NO_3 is lower than Cl	this work
7	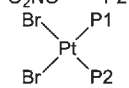	2.280[a]	Pt–P bonds longer than in **1**, **3** and **5**	this work
11	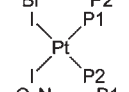	2.285[a]	Pt–P bonds longer than in **1**, **3**, **5** and **7**	this work
13	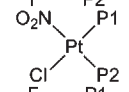	2.260(1) 2.243(1)	Pt–P1 slightly shorter than in **1** but longer than in **2** and **4**: *cis* influence of NO_2 lower than Cl, but higher than AcO and NO_3 Pt-P2 shorter than in **1**: *trans* influence of NO_2 lower than Cl	this work
23	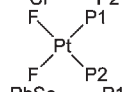	2.225[a]	shortest Pt-P bonds	33
26	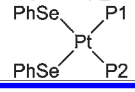	2.292[a]	Pt–P bonds longer than in **1**, **3**, **5**, **7** and **11**	34

[a] Mean value.

Table 6. Selected Bond Lengths (Å) and Torsion Angles (deg) in Computed B3LYP/def2-SVP *cis*-[$PtX_2(PPh_3)_2$] Compounds

X	Pt−P1	Pt−P2	Pt−X1	Pt−X2	A[a]	B[b]
NO_3 (**5**)	2.301	2.312	2.094	2.091	8.8	−48.7
AcO (**3**)	2.306	2.318	2.079	2.072	−4.7	49.0
Cl (**1**)	2.320	2.337	2.393	2.368	−5.7	50.7
Br (**7**)	2.333	2.354	2.534	2.506	−5.1	50.9
I (**11**)	2.353	2.375	2.739	2.707	−3.8	51.4
NO_2 (**14**)	2.370	2.397	2.107	2.090	−13.8	−38.8
Ph (**22**)	2.459	2.459	2.069	2.069	29.7	30.1

[a] Lowest X2−Pt−P1−**C** torsion angle (phosphine A of Scheme 1). [b] Lowest X1−Pt−P2−**C** torsion angle (phosphine B of Scheme 1).

Table 7. Selected Bond Lengths (Å) and Torsion Angles (deg) in Computed B3LYP/def2-SVP *cis*-[$PtClX(PPh_3)_2$] Compounds

X	Pt−P1	Pt−P2	Pt−O/N/C	Pt−Cl	A[a]	B[b]
NO_3 (**4**)	2.322	2.311	2.092	2.383	−3.3	52.4
AcO (**2**)	2.318	2.319	2.072	2.388	−2.7	48.7
Cl (**1**)	2.320	2.337	2.368	2.393	−5.7	50.7
Br (**6**)	2.319	2.352	2.503	2.394	−2.7	50.7
I (**10**)	2.318	2.374	2.699	2.398	−1.5	50.8
NO_2 (**13**)	2.314	2.396	2.076	2.393	−11.1	−48.6
Ph (**21**)	2.293	2.515	2.052	2.399	11.2	−48.3

[a] Lowest Cl−Pt−P2−**C** torsion angle (phosphine B of Scheme 1). [b] Lowest X−Pt−P1−**C** torsion angle (phosphine A of Scheme 1).

considering the mixed ClX complexes: Ph > NO_2 > I > Br > Cl > AcO ≥ NO_3.

It is interesting to analyze the case of the ClPh complex (**21**), essentially the only one where the structural cis influence is detectable and compare it with the Cl_2 (**1**) and the Ph_2 (**22**) complexes. Comparison with Cl_2 indicates that the Pt−P1 bond length in ClPh is shortened by 0.027 Å, showing the lower cis influence of Ph with respect to Cl. On the other hand, Pt−P2 is elongated by 0.178 Å, due to the much higher trans influence of Ph with respect to Cl. Such elongation shows also the lower magnitude of the cis over the trans influence of Ph. Comparison with the Ph_2 complex shows that Pt−P1 in ClPh is shortened by 0.166 Å and Pt−P2 is elongated by 0.056 Å, due to the substitution of a Ph with a lower trans-influent and higher cis-influent Cl ligand. As a consequence of such different cis/trans influence of the two ligands, the Pt−P bond lengths in the ClPh complex present a very large asymmetry, differing by 0.222 Å.

Spectroscopic Cis and Trans Influences. Table 8 reports the $^{31}P\{^1H\}$ NMR spectra of some *cis*-[$PtX_2(PPh_3)_2$] and *cis*-[$PtXY(PPh_3)_2$] complexes. In the case of the latter, assignment of the two resonances was made by comparison of their chemical shifts with those of the X_2 derivatives. As a proof of correctness, in the case of *cis*-[$PtCl(AcO)(PPh_3)_2$] (**2**) we have performed a P−H HMBC (heteronuclear multibond correlation) experiment which showed a cross-peak between the resonance of the acetato protons and the P resonance at 3.1 ppm, in agreement with the assignment of this resonance to P trans to AcO.

If we shall follow, again, a first approach considering only the X_2 complexes, and neglecting, in the first approximation, the cis influence, or assuming that it has an irrelevant weight, the $^1J_{PtP}$ values of these complexes

give the "apparent" order of trans influence (increasing coupling constants, decreasing trans influence):

$$\mathrm{Ph} > \mathrm{Me} > \mathrm{SPh} > \mathrm{SePh} > \mathrm{NO_2} > \mathrm{I} > \mathrm{N_3} > \mathrm{Br} > \mathrm{Cl} > \mathrm{AcO} > \mathrm{CF_3COO} > \mathrm{F} > \mathrm{NO_3}$$

However, inspection of the data of the mixed XY complexes shows that the cis influence must not be neglected. For instance, let us consider *cis*-[PtCl(NO_3)(PPh_3)$_2$] (**4**): while $^1J_{PtP2}$ is higher than that of **1**, in agreement with the fact that the nitrato ligand displays a trans influence lower than that of Cl, $^1J_{PtP1}$ is also higher than that of **1**, suggesting that the low cis influence[8] of NO_3 is operative.

In our previous paper on *trans*-[PtXY(PPh_3)$_2$],[8] we confirmed the already noticed[6a,38,45] additivity of the contributions of the cis influences to $^1J_{PtP}$. We tried and apply an additive scheme in this case to both cis and trans influences.

The coupling constants $^1J_{PtP}$ of each P nucleus in compounds *cis*-[PtX$_2$(PPh_3)$_2$] and *cis*-[PtXY(PPh_3)$_2$] can be considered as the sum of all the contributions given by the cis and trans ligands PPh_3, X and/or Y to a basic value (N), considered as a constant starting point for this class of square planar, neutral Pt(II) compounds, and which represents the energy of the interaction between the nuclear spins of Pt and P. This value is perturbed by the presence of the ligands. If we call a, b, c, etc. the cis contributions and α, β, χ, etc. the trans contributions (Here, a, α for PPh_3; b, β, for Cl; c, χ, for AcO; d, δ, for NO_3; e, ε for Br; f, ϕ for I; g, γ for NO_2; h, η for PhS; i, ι for F_3CS; l, λ, Me; m, μ, Ph. See Table 8.), the Pt−P coupling constant of **1** is

$$N + a + b + \beta = 3673 \text{ Hz} \quad (1)$$

the $^1J_{PtP}$ values of *cis*-[PtCl(NO_3)(PPh_3)$_2$] (**4**) are

$$N + a + d + \beta = 3842 \text{ Hz (for P1)} \quad (2)$$

and

$$N + a + b + \delta = 3858 \text{ Hz (for P2)} \quad (3)$$

whereas the Pt−P coupling constant of both P nuclei of *cis*-[Pt(NO_3)$_2$(PPh_3)$_2$] (**5**) is

$$N + a + d + \delta = 4013 \text{ Hz} \quad (4)$$

Subtracting 1 − 2, or 3 − 4, will reduce to $b - d$, the difference between the cis contributions of NO_3 and Cl. The contributions of Cl cannot be obtained with the present treatment, but they can be used as references, thus d and δ are the cis and trans contributions of NO_3 *relative* to Cl. Performing similar calculations for all complexes, we obtain the contributions of the two influences of the various ligands. The equations considered and the results are reported in Table 8.

Note that we obtain two similar but different values for each contribution, depending on the subtraction considered. For instance, for d, 1 − 2 = −169 Hz, whereas 3 − 4 = −155 Hz. These differences are too large to be only due to the reproducibility of the measure of the coupling constants (±3 Hz). We believe that these differences arise mainly from the fact that both subtractions reduce to $b - d$, eliminating N and especially a, whose constancy is a working hypothesis, useful for the present treatment. In particular, the value of N can be safely considered constant as explained above, while, on the contrary, the values of a (and also α) may depend on the overall coordination set and can vary according to the nature of the other ligands (X and Y). In fact, while d obtained from 1 − 2 is referred to the Cl_2 complex, subtracting 3 − 4 gives d referred to the mixed Cl(NO_3) complex. Thus the contributions of the phoshines, a, and of the ligand X/Y depend not only on their nature, but also on that of all their neighbors. The additivity scheme must therefore be applied with great care in the present case, where both the cis and trans influences are taken into account.

Despite this drawback, however, some consistency is obtained if we refer to a homogeneous class of compounds, such as the ClX derivatives. In this case, the values of c and χ, d and δ, etc. discriminate between the cis and trans influences and give a sequence of both and, more importantly, an insight into their relative weights. Since we have subtracted 1 − 2, 3 − 4, etc., negative values mean higher contributions to $^1J_{PtP}$ of X compared to Cl and then a lower influence.

Under the above-discussed approximations, we obtain the following series:

cis

$$f < e < b < i < d \approx h < g < c < l, m$$

$$\mathrm{I} > \mathrm{Br} > \mathrm{Cl} > \mathrm{SCF_3} > \mathrm{NO_3} \approx \mathrm{SPh} > \mathrm{NO_2} \approx \mathrm{AcO} > \mathrm{Me} > \mathrm{Ph}$$

trans

$$\lambda, \mu < \eta < \gamma < \iota < \beta \approx \varepsilon < \phi < \chi < \delta$$

$$\mathrm{Ph, Me} > \mathrm{SPh} > \mathrm{NO_2} > \mathrm{SCF_3} > \mathrm{AcO} > \mathrm{Br} \approx \mathrm{Cl} > \mathrm{I} > \mathrm{NO_3}$$

Some points are worthy of discussion:

(i) There is a span of approximately 2000 and 1000 Hz for the trans and cis influences, respectively. The latter, therefore, has a lower weight, but our data show that it is by no means irrelevant (in some cases it appears to be even higher).

(ii) We confirm the almost opposite trend of the cis and trans influence series.[4]

(38) Yamashita, F.; Kuniyasu, H.; Terao, J.; Kambe, N. *Inorg. Chem.* **2006**, *45*, 1399–1404.
(39) Kirij, N. V.; Tyrra, W.; Naumann, D.; Pantenburg, I.; Yagupolskii, Yu. L. *Z. Anorg. Allg. Chem.* **2006**, *632*, 284–288.
(40) Cobley, C. J.; Pringle, P. G. *Inorg. Chim. Acta* **1997**, *265*, 107–115.
(41) Haar, C. M.; Nolan, S. P.; Marshall, W. J.; Moloy, K. G.; Prock, A.; Giering, W. P. *Organometallics* **1999**, *18*, 474–479.
(42) Eaborn, C.; Odell, K. J.; Pidcock, A. *J. Chem. Soc., Dalton Trans.* **1978**, 357–368.
(43) Braterman, P. S.; Cross, R. J.; Young, G. B. *J. Chem. Soc., Dalton Trans.* **1977**, 1892–1897.
(44) Kreutzer, P. H.; Schorpp, K. T.; Beck, W. *Z. Naturforsch.* **1975**, *30b*, 544–549.
(45) Additivity has been noted also for the kinetic cis effect, for example: Jaganyi, D.; Hofmann, A.; van Eldik, R. *Angew. Chem., Int. Ed.* **2001**, *40*, 1680–1683.

Table 8. ^{31}P NMR Data for Some *cis*-[$PtX_2(PPh_3)_2$] and *cis*-[$PtXY(PPh_3)_2$] Complexes[a]

	compound	δ_P (ppm)	$^1J_{PtP}$ (Hz)	*cis* and *trans* contributions[b]			ref
				equation	*cis* contribution (Hz)	*trans* contribution (Hz)	
1	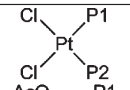	14.9	3673	$N + a + b + \beta$	–	–	this work
2	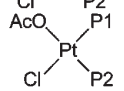	18.3	3956	$N + a + c + \beta$	$b - c = -283$		this work
		3.1	3560	$N + a + b + \chi$		$\beta - \chi = 113$	
3	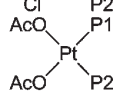	5.9	3826	$N + a + c + \chi$	$b - c = -266$	$\beta - \chi = 130$	12, this work
4	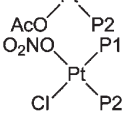	17.6	3842	$N + a + d + \beta$	$b - d = -169$		this work
		2.7	3858	$N + a + b + \delta$		$\beta - \delta = -185$	
5	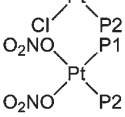	3.6	4013	$N + a + d + \delta$	$b - d = -155$	$\beta - \delta = -171$	12,37
6	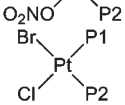	15.3	3618	$N + a + e + \beta$	$b - e = 55$		this work
		13.6	3665	$N + a + b + \varepsilon$		$\beta - \varepsilon = 8$	
7	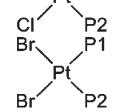	14.3	3614	$N + a + e + \varepsilon$	$b - e = 51$	$\beta - \varepsilon = 4$	this work
8	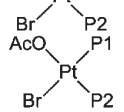	18.8	3907	$N + a + c + \varepsilon$	$e - c = -293$	$\varepsilon - \chi = 76$	this work
		2.0	3538	$N + a + e + \chi$	$e - c = -288$	$\varepsilon - \chi = 81$	
9	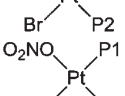	17.8	3790	$N + a + d + \varepsilon$	$e - d = -176$	$\varepsilon - \delta = -212$	this work
		1.5	3826	$N + a + e + \delta$	$e - d = -187$	$\varepsilon - \delta = -223$	
10	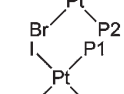	13.7	3420	$N + a + f + \beta$	$b - f = 253$	–	this work
		11.6	3683	$N + a + b + \phi$	–	$\beta - \phi = -10$	
11	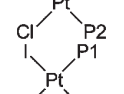	11.9	3455	$N + a + f + \phi$	$b - f = 228$	$\beta - \phi = -35$	this work
12	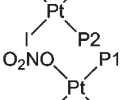	15.5	3596	$N + a + d + \phi$	$f - d = -141$	$\phi - \delta = -364$	this work
		–0.5	3819	$N + a + f + \delta$	$f - d = -194$	$\phi - \delta = -417$	
13	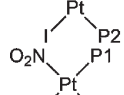	12.2	3949	$N + a + g + \beta$	$b - g = -276$	–	this work
		–0.5	2883	$N + a + b + \gamma$	–	$\beta - \gamma = 790$	
14	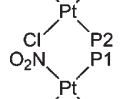	–1.3	3148	$N + a + g + \gamma$	$b - g = -265$	$\beta - \gamma = 801$	this work
15	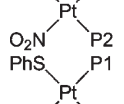	20.1[c]	3840	$N + a + h + \beta$	$b - h = -167$	–	38
		21.6[c]	2676	$N + a + b + \eta$	–	$\beta - \eta = 997$	
16	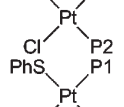	23.8[c]	2880	$N + a + h + \eta$	$b - h = -204$	$\beta - \eta = 960$	38
17	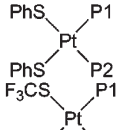	14.8[d]	3725	$N + a + i + \beta$	$b - i = -52$	–	39
		17.6[d]	3033	$N + a + b + \iota$	–	$\beta - \iota = 640$	
18	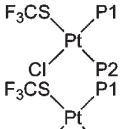	17.8[d]	3147	$N + a + i + \iota$	$b - i = -114$	$\beta - \iota = 578$	39
19	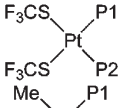	22.3	4500	$N + a + l + \beta$	$b - l = -827$	–	40
		27.1	1727	$N + a + b + \lambda$	–	$\beta - \lambda = 1946$	
20	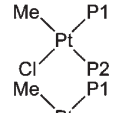	27.7[d]	1900	$N + a + l + \lambda$	$b - l = -173$	$\beta - \lambda = 2600$	41
21	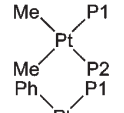	17.2[e]	4500	$N + a + m + \beta$	$b - m = -827$	–	42
		21.5[e]	1560	$N + a + b + \mu$	–	$\beta - \mu = 2133$	
22	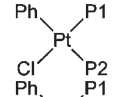	18.3	1763[42] 1748[43]	$N + a + m + \mu$	$b - m = -203$	$\beta - \mu = 2737$	42,43

Table 8. Continued

	compound	δ_P (ppm)	$^1J_{PtP}$ (Hz)	*cis* and *trans* contributions[b]			ref
				equation	*cis* contribution (Hz)	*trans* contribution (Hz)	
23	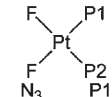	5.0	3966	–	–	–	33
24	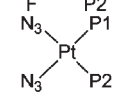	11.5[e]	3540	–	–	–	44
25	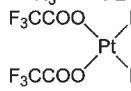	4.4	3933	–	–	–	12
26	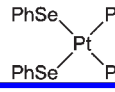	19.1[f]	2968	–	–	–	34

[a] $CDCl_3$ solutions, unless otherwise stated; δ_P values in parts per million versus aqueous H_3PO_4 (for compounds **21**, **22**, and **24**, different references were used, and here, the δ_P values have been recalculated to agree with all other data); $^2J_{PP}$ are in the 12−20 Hz range, see the Experimental Section. [b] *a*, *b*, *c*, etc. are the contributions of the cis ligands; α, β, χ, etc. are the contributions of the trans ligands (*a*, α = PPh_3; *b*, β = Cl; *c*, χ = AcO; *d*, δ = NO_3; *e*, ε = Br; *f*, φ = I; *g*, γ = NO_2; *h*, η = PhS; *i*, ι = F_3CS; *l*, λ = Me; *m*, μ = Ph); and *N* is the basic value; such contributions are given mainly as the difference from Cl_2. [c] C_6D_6. [d] CD_2Cl_2. [e] CH_2Cl_2. [f] C_6H_6.

(iii) The cis influence series is similar to that obtained in the previous work,[8] the positions of NO_2 and AcO are inverted, but the contributions of these ligands are very similar in both cis and trans derivatives.

(iv) The values of the cis contributions obtained here are about 30% higher than those calculated in the previous paper[8] from the Pt−P coupling constants of the *trans*-[PtXY(PPh_3)$_2$] isomers, showing that the actual contribution of a given ligand depends on the system under study.

(v) The trans influence series parallels that obtained above considering only the X_2 complexes, with the notable exception of the position of AcO, which becomes higher in the series when the cis influence is taken into account, clear-cut evidence that the cis influence cannot be neglected.

(vi) The trans sequence of the halides (Br ≥ Cl ≥ I) is unexpected, but their contributions are similar and low and can be affected by some uncertainty. The sequence I > Br > Cl seems well established in the literature,[46] but such reports do not take into account the contribution of the cis influence. While the order (I > Br > Cl) of the kinetic trans effect is well-established,[47,48] the fact that, on the contrary and according to our results, their trans influences are similar stresses the different significance and origin (ground state versus transition state stabilization) of the two phenomena.[49]

(vii) The cis contributions of the halides are higher than their trans contributions. As argued in the previous paper,[8] the cis influence of a ligand is related to the lowering of the positive charge on Pt induced by that ligand. The halides display a high cis influence because, being both σ and π donor,[50] they decrease the positive charge on Pt efficaciously (as shown below), decreasing the P → Pt donation.[51]

(viii) There is no net parallelism between the structural and spectroscopic series, as a confirmation of the well-known dependence on the physical method used to establish such series.[4,46]

In order to check the general validity of the additivity of the contributions of the various X ligands calculated with respect to *cis*-[PtClX(PPh_3)$_2$] (Table 8), let us take into consideration a compound without Cl as a ligand, *cis*-[PtBr(AcO)(PPh_3)$_2$] (**8**). Referring to compounds **3** and **7**, we obtain $\varepsilon - \chi = 76$ or 81 (confirming the higher trans influence of Br than AcO) and $e - c = -293$ or -288 (confirming the lower cis influence of Br than AcO). However, if the contributions are calculated using compound **1** as reference, we obtain $\varepsilon - \chi = (\beta - \chi) - (\beta - \varepsilon) = (130) - (8) = 122$ Hz and $e - c = (b - c) - (b - e) = (-266) - (55) = -321$ Hz. Although the calculated values of χ and *c* reflect the general trend, they are rather different. The same discrepancies are obtained with the other compounds without Cl, **9** and **12**. This fact clearly confirms that the actual contributions of the ligands depend from the nature of its neighbor Y, indicating that there is cooperation between the two cis ligands.

Natural Bond Orbital (NBO) Analysis. To give a possible explanation of the different trans/cis influence of the

(46) See, for instance, Bennett, M. A.; Bhargava, S. K.; Privér, S. H.; Willis, A. C. *Eur. J. Inorg. Chem.* **2008**, 3467–3481, and references therein.

(47) Cotton, F. A.; Wilkinson, G.; Gaus, P. L. *Basic Inorganic Chemistry*, 3rd ed.; John Wiley and Sons: New York, 1995.

(48) The rather higher trans effect of I compared with Cl is the basis for a stereoselective synthesis of cisplatin (*cis*-[$PtCl_2(NH_3)_2$]): [$PtCl_4$]$^{2-}$ is first allowed to react with KI to give [PtI_4]$^{2-}$ which, upon treatment with ammonia, gives *cis*-[$PtI_2(NH_3)_2$] in very high isomeric purity. *cis*-[$PtCl_2(NH_3)_2$] is then obtained by metathesis reactions. See: Dhara, S. C. *Indian J. Chem.* **1970**, *8*, 193–194. The direct reaction of [$PtCl_4$]$^{2-}$ with ammonia gives cisplatin contaminated by the trans isomer.

(49) To our knowledge there is at least one example in which the order of the trans influence is opposite to that of the trans effect, see: Wendt, O. F.; Elding, L. I. *J. Chem. Soc., Dalton Trans.* **1997**, 4725–4731.

(50) Bridgeman, A. J.; Gerloch, M. *J. Chem. Soc., Dalton Trans.* **1995**, 197–204.

(51) Strong donor ligands display also a strong (kinetic) cis effect because, lowering the positive charge on Pt, they reduce its electrophilicity. See: (a) Hofmann, A.; Dahlernburg, L.; van Eldik, R. *Inorg. Chem.* **2003**, *42*, 6528–6538. (b) Jaganyi, D.; Reddy, D.; Gertenbach, J. A.; Hofmann, A.; van Eldik, R. *Dalton Trans.* **2004**, 299–304.

Table 9. Pt and P Natural Orbitals Involved in the Pt−P Bonds and Natural Charges on Pt, q_{Pt} (in *e*), in Computed B3LYP/def2-SVP *cis*-[$PtX_2(PPh_3)_2$] Compounds

X	bond orbital Pt−P1	bond orbital Pt−P2	q_{Pt}
I (**11**)			0.06
Br (**7**)	$33.72\%(sd^{1.06})_{Pt} + 66.28\%(sp^{2.94})_{P1}$	$32.98\%(sd^{1.08})_{Pt} + 67.02\%(sp^{2.96})_{P2}$	0.14
Cl (**1**)	$33.51\%(sd^{1.06})_{Pt} + 66.49\%(sp^{2.93})_{P1}$	$32.84\%(sd^{1.10})_{Pt} + 67.16\%(sp^{2.95})_{P2}$	0.20
AcO (**3**)	$31.47\%(sd^{1.08})_{Pt} + 68.53\%(sp^{2.88})_{P1}$	$30.82\%(sd^{1.10})_{Pt} + 69.18\%(sp^{2.91})_{P2}$	0.45
NO_3 (**5**)	$32.44\%(sd^{1.07})_{Pt} + 67.56\%(sp^{3.01})_{P1}$	$32.01\%(sd^{1.11})_{Pt} + 67.99\%(sp^{3.05})_{P2}$	0.44
NO_2 (**14**)	$30.46\%(sd^{1.12})_{Pt} + 69.54\%(sp^{3.08})_{P1}$	$29.45\%(sd^{1.10})_{Pt} + 70.55\%(sp^{3.10})_{P2}$	0.27
Ph (**22**)			0.19

Table 10. Pt and P Natural Orbitals Involved in the Pt−P Bonds and Natural Charges on Pt, q_{Pt} (in *e*), in Computed B3LYP/def2-SVP *cis*-[$PtClX(PPh_3)_2$] Compounds

X	bond orbital Pt−P1	bond orbital Pt−P2	q_{Pt}
I (**10**)	$33.13\%(sd^{1.10})_{Pt} + 66.87\%(sp^{2.83})_{P1}$		0.13
Br (**6**)	$33.51\%(sd^{1.10})_{Pt} + 66.49\%(sp^{2.88})_{P1}$	$33.06\%(sd^{1.04})_{Pt} + 66.94\%(sp^{3.00})_{P2}$	0.17
Cl (**1**)	$33.51\%(sd^{1.06})_{Pt} + 66.49\%(sp^{2.93})_{P1}$	$32.84\%(sd^{1.10})_{Pt} + 67.16\%(sp^{2.95})_{P2}$	0.20
AcO (**2**)	$32.98\%(sd^{1.00})_{Pt} + 67.02\%(sp^{2.98})_{P1}$	$31.56\%(sd^{1.18})_{Pt} + 68.44\%(sp^{2.88})_{P2}$	0.34
NO_3 (**4**)	$33.24\%(sd^{0.99})_{Pt} + 66.76\%(sp^{3.06})_{P1}$	$32.60\%(sd^{1.19})_{Pt} + 67.40\%(sp^{2.94})_{P2}$	0.32
NO_2 (**13**)	$31.92\%(sd^{0.85})_{Pt} + 68.08\%(sp^{3.00})_{P1}$		0.25
Ph (**21**)	$31.71\%(sd^{0.85})_{Pt} + 68.29\%(sp^{2.69})_{P1}$		0.21

ligands, we have performed a natural bond orbital (NBO) analysis[25] on the optimized structures discussed in a previous section. We were interested, in particular, to analyze the bonding orbitals used by Pt and P in the Pt−P bonds. One bond coupling constants are in fact supposed to be dominated by the Fermi contact term,[52] which takes into account the s-character of the bonding orbitals and the electron densities of the *ns* valence orbitals at the nuclei. In the complexes studied in this paper, both the s-character of the hybrid orbitals and the electron density of the $3sp^3$ orbital of phosphorus and sd of platinum have been considered to be rather similar throughout,[3,4,7b,7c,53] but we wanted to have a deeper look at these points, since these factors can be related to the different trans and cis influences of the ligands in the complexes examined.

The results, reported in Tables 9 and 10 for *cis*-[$PtX_2(PPh_3)_2$] and *cis*-[$PtClX(PPh_3)_2$] complexes, respectively, are far to be conclusive, also because in the cases of the long Pt−P bonds, the involved orbitals are interpreted by NBO analysis as lone pairs rather than bonding orbitals, so they have not been included in Tables 9 and 10. Some observations are, however, noteworthy:

(i) For *cis*-[$PtX_2(PPh_3)_2$] compounds (Table 9), the s-character of both P and Pt orbitals involved in the Pt−P bonds is almost the same. Averaging on Pt−P1 and Pt−P2 bonds, the hybridization degrees of sd^x and sp^y orbitals vary from $x = 1.07$ to 1.11 and from $y = 2.90$ to 3.09, respectively, and in particular, they do not show any clear correlation with the structural and spectroscopic influences reported above. It therefore seems that for such complexes the s-character of Pt and P orbitals involved in the Pt−P bonds does not represent a relevant factor in explaining the trans influence of the ligands.

(ii) In *cis*-[$PtClX(PPh_3)_2$] complexes (Table 10), on the other hand, the s-character of the Pt−P1 bond orbitals shows a clear trend, increasing in the order I ≅ Br < Cl < AcO < NO_3 < NO_2 ≅ Ph for the sd^x orbitals of Pt and decreasing in the same order (with the exception of NO_2 and Ph) for the sp^y orbitals of P. As a result, the total *s*-contribution to the Pt−P1 bond is nearly constant and equal to 33% for all ligands, except for NO_2 (34%) and Ph (36%). The slight increase of the s-character of Pt−P1 for X = NO_2 and Ph explains its shortening with respect to the value of the other complexes, as obtained from geometry optimization calculations. It is to be noted that the sequence of increasing s-character of the sd^x orbitals of Pt parallels approximately the order of cis influence obtained by NMR measurements reported here and in the previous work[8] (the order of AcO and NO_3 is inverted): the greater the s-character of such orbitals, the greater the $^1J_{PtP1}$ value. It therefore appears that the cis influence is principally related with the s-character of the Pt valence orbitals. It is also to be stressed that, while the cis influence cannot be completely revealed by looking at the Pt−P1 bond length of the optimized structures of the mixed complexes, it manifests itself clearly in the nature of the associated bonding orbitals.

(iii) As for the Pt−P2 bond orbitals of *cis*-[$PtClX(PPh_3)_2$] complexes (Table 10), where the trans influence of the ligands comes into play, the s-character displays an opposite trend of the sd^x orbitals, as it decreases in the order Br > Cl > AcO > NO_3, while the sp^y orbitals on the P2 atom do not show a clear trend. As a result, the total s-contribution to the Pt−P2 bond shows only a slight decrease from Br (33%) to NO_3 (32%). Such an outcome, as discussed in previous point i, confirms that other factors

(52) Jameson, C. In *Multinuclear NMR*; Mason, J., Ed.; Plenum Press: New York, 1987; pp 89−131.

(53) For instance: (a) Allen, F. H.; Pidcock, A. *J. Chem. Soc.* (*A*) **1968**, 2700–2704. (b) Allen, F. H.; Sze, S. N. *J. Chem. Soc.* (*A*) **1971**, 2054–2056.

seem principally responsible of the trans influence of the ligands.

Further information derived from the natural orbital analysis of electron density concerns the atomic charges, whose values for Pt, q_{Pt}, are also reported in Tables 9 and 10 for *cis*-[$PtX_2(PPh_3)_2$] and *cis*-[$PtClX(PPh_3)_2$] complexes, respectively. These quantities, which reflect the total electron density associated with the Pt atom show an interesting trend, which is in good agreement with what argued on the basis of the NMR measurements. The lowest positive charges are in fact obtained with the halides, in the order I < Br < Cl, i.e. for the ligands which display the highest cis influences, while the largest q_{Pt} values correspond to the low cis-influencing ligands AcO and NO_3. Low positive charges on Pt are also obtained in the complexes with NO_2 and Ph, for which a larger covalence degree of the Pt−X bond can be expected. All these changes in q_{Pt} point out the relative importance of also the electrostatic contribution to the Pt−P interaction. In the case of halides and anionic ligands (NO_3, AcO), such contribution cannot be neglected, while it appears less relevant for complexes with metal−ligand bonds with a higher degree of covalency (ligand = Ph, NO_2).

Conclusions

We have shown that in compounds of the type *cis*-[$PtXY(PPh_3)_2$] the cis and trans influences cooperate in determining the experimental bond lengths and one bond coupling constants $^1J_{PtP}$ of the Pt−P bonds. We have also obtained an insight on the magnitude of both influences from the values of such constants and found that the weight of the cis influence is not irrelevant and must be taken into account in establishing the trans influence scale.

A commonly accepted interpretation of the trans influence is that two ligands trans to each other compete for a same hybrid orbital, which spans across the metal atom. As for the cis influence, it has been rationalized assuming that, in Pt(II), Pt−P back-donation can be considered little relevant,[54] therefore, the Pt−P bonds can be described mainly as donation from an sp^3 orbital of P to an hybrid orbital of Pt. Under this approximation, the Pt−P bonds become weaker as the metal atom becomes less positively charged,[8] a trend confirmed by natural bond orbital analysis on the B3LYP/def2-SVP optimized structures. Such a computational study has also pointed out that the s-character of Pt and P hybrid orbitals involved in the Pt−P bonds can be related to the cis influence of the ligands, while it does not represent a relevant factor in explaining their trans influence.

It is interesting to compare the results here presented with those reported by our group in the previous paper,[8] where we have evaluated the cis influences of some anionic ligands analyzing the $^1J_{PtP}$ values of the trans isomers of some compounds of the present study. Although the cis influence series are similar, the magnitudes calculated from the cis isomers are about 30% higher than those obtained previously. Clearly these weights depend on the system under study; for instance in the X_2 complexes, a ligand, say AcO, is cis to a phosphine in the trans isomer, but cis to another AcO in the cis derivative.

A related point is worth noting. As stated above, the weights of both influences of a given ligand depend not only on its nature but also on its neighborhood; for instance, the weight of AcO in a mixed complex X(AcO) varies according to the ligand X, suggesting a synergism between the two cis ligands. One can speculate that, since these weights are in Hz, they describe how a ligand X perturbs (modifies) the energy of the interaction between the nuclear spins of Pt and P. Clearly such perturbation must depend not only on the nature of X but also on its environment, the charge on Pt, etc., ultimately on the overall coordination set.

Despite this limitation, however, both cis and trans influences have been clearly detected, although precise quantitative evaluation of their magnitudes requires further studies, which we aim to undertake in the near future.

Acknowledgment. This work has been supported by the Ministero dell'Università e della Ricerca Scientifica e Tecnologica.

Supporting Information Available: X-ray crystallographic data of compounds **2**, **3**·0.25H_2O, **4**·$CHCl_3$, **5**·CH_2Cl_2, **5**·$CHCl_3$, **7**, **11**·H_2O, and **13** in CIF format and figures of the crystal structures of the compounds **2**, **4**·$CHCl_3$, **5**·CH_2Cl_2, **5**·$CHCl_3$, and **7**. This material is available free of charge via the Internet at http://pubs.acs.org.

(54) In Pt(II) complexes, there is a neat correlation between $^1J_{PtP}$ and the donor power of aryl phosphines, suggesting that π back-donation to P is negligible, see ref 40.